

Isothermal spheres in general relativity and Hořava-type gravity

Nahomi Kan*

National Institute of Technology, Gifu College, Motosu-shi, Gifu 501-0495, Japan

Kiyoshi Shiraishi†

*Faculty of Science, Yamaguchi University,
Yamaguchi-shi, Yamaguchi 753-8512, Japan*

We construct a toy model for isothermal spheres in Hořava's gravity, which includes Einstein's gravity if a parameter is appropriately chosen. The equations for the isothermal spheres are derived from the partition function of the gravitating particle system. We confirm that the Newtonian limit of the system coincides with the model of the well-known isothermal sphere. The stability of the isothermal sphere is found to be sensitive to the energy density at the center of the sphere.

arXiv:2010.00173v1 [gr-qc] 1 Oct 2020

* kan@gifu-nct.ac.jp

† shiraish@yamaguchi-u.ac.jp

I. INTRODUCTION

Although an isothermal sphere is a very ideal object, it has been considered as a Newtonian body of a self-gravitating gas as a model, not only for a star [1] but for a stellar cluster and a galaxy [2] for a long time in the past. The isothermal sphere has the asymptotic density proportional to r^{-2} where r is the distance from the center of a sphere, if the distance is sufficiently large.¹ At the same time, the isothermal sphere is a nice theoretical laboratory for the self-gravitational system, which has a novel thermodynamical behavior [3–5].

Now a day, the dark matter problem in the universe has been widely discussed, and several proposals have appeared with candidates from the particle physics [6, 7]. On the other hand, modified gravity has been proposed as an alternative to the dark matter [8, 9]. Above all, attempts to reproduce the density profiles of the galaxies exist with both approaches, but at present they have not been firmly resolved. There is room for both modified gravity and unknown matter to solve the problem.

The modification of the theory of gravity is also required because of its consistency as a complete quantum theory, and various attempts have been made to date focusing on the behavior of gravity in the UV region. In this paper, we investigate the properties of the isothermal sphere in Hořava gravity [10, 11], which is one of the modified gravity theories expected to be a UV complete theory. Considering the isothermal gas sphere has the merit that it is easy to understand whether the relativistic or modified theory of gravity will be crucial or not for certain features of the isothermal sphere, which have been investigated in the Newtonian systems. The present study allows us to better understand, in addition to the structure and nature of self-gravitational system, the modified gravity theories and the nature of coupling to matters in a peculiar situation.²

One may suspect that the density profile of spheres at large scale can be affected by the modification, which is only expected at high energy region. It has however been reported [13] that the structure of isothermal spheres in the ‘softened’ gravity is very different from the Newtonian isothermal spheres. The softened Newton gravity has a small constant scale in the gravitational potential. Thus, aside from the magnitude of deviations, it is worth trying to figure out whether some difference appears in the structure of isothermal spheres in general relativity and modified theory of gravity. Furthermore, it should be mentioned

¹ Such a density profile can explain the flat rotation curves found in many galaxies.

² The studies on stellar structure models in modified gravitational theories to date are reviewed in [12].

that analyses of models of celestial bodies and galaxies according to the fractional law of gravitation has also appeared recently [14–16], and that the higher-derivative modification of Newton’s law is also considered more recently [17].

The present paper is organized as follows: in Sec. II we introduce the Hořava-type gravity we will consider in this paper; in Sec. III the partition function of relativistic particles coupled with the metric is discussed; in Sec. IV we extract the classical equations of motion for isothermal spheres from the total partition function of the gravitating system; in Sec. V we illustrate the results for the isothermal spheres in Einstein’s gravity and in Hořava’s gravity; Sec. VI constitutes the conclusions.

II. HOŘAVA-TYPE GRAVITY WHICH WE CONSIDER IN THE PRESENT WORK

Since its proposal by Hořava [10, 11], there are now various versions of the Hořava gravity model [18]. In this paper, we pick out the simplest model among them [19–21]. We wish to study an ideal isothermal model at this first step, and thus deal with the simplified Hořava gravity model in this paper. However, its generalization will be straightforward. The model can be regarded as a lowest-order corrected higher-derivative theory of gravity beyond the Einstein gravity.

The Hamiltonian formalism is adopted for the system in the present analysis. We start with the ADM line element [22],

$$ds^2 = -N^2 dt^2 + \tilde{g}_{ij}(dx^i + N^i dt)(dx^j + N^j dt), \quad (2.1)$$

where N is the lapse function, N^i ($i, j = 1, 2, 3$) is the shift vector, and \tilde{g}_{ij} is the spatial metric. The Hamiltonian is then written in the form

$$H = \int d^3x \sqrt{\tilde{g}} (N\mathcal{H} + N^i\mathcal{H}_i), \quad (2.2)$$

where \tilde{g} is the determinant of the matrix elements \tilde{g}_{ij} . Here, the Hamiltonian constraint \mathcal{H} and the momentum constraint \mathcal{H}_i are given in the $z = 2$ model of the Hořava gravity [10, 19]

$$\mathcal{H} = \frac{\kappa^2}{2\sqrt{\tilde{g}}} \left[\pi^{ij}\pi_{ij} - \frac{\lambda}{3\lambda - 1}(\pi_i^i)^2 \right] - \mu^3 \tilde{R} - \frac{\kappa^2 \mu^2 (4\lambda - 1)}{32(3\lambda - 1)} \tilde{R}^2 + \frac{\kappa^2 \mu^2}{8} \tilde{R}^{ij} \tilde{R}_{ij}, \quad (2.3)$$

$$\mathcal{H}_i = -2\nabla^j \pi_{ij}, \quad (2.4)$$

with π^{ij} being the conjugate momentum of \tilde{g}_{ij} , \tilde{R} and \tilde{R}_{ij} being the scalar curvature and the Ricci tensor constructed from \tilde{g}_{ij} , respectively. Here, ∇_i denotes the three-dimensional covariant derivative and the parameters κ and λ are constants. In the case of $\lambda = 1$, the Hamiltonian density \mathcal{H} becomes [19–21]

$$\mathcal{H} = \frac{\kappa^2}{2\sqrt{\tilde{g}}} \left[\pi^{ij}\pi_{ij} - \frac{1}{2}(\pi_i^i)^2 \right] - \mu^3 \left[\tilde{R} - \frac{2}{\omega} \left(\tilde{R}^{ij}\tilde{R}_{ij} - \frac{3}{8}\tilde{R}^2 \right) \right], \quad (2.5)$$

with $\omega \equiv \frac{16\mu}{\kappa^2}$. Hereafter, we consider this Hořava-type gravity model.

The higher-order terms are important when discussing UV completion of quantum gravity in general. We would like to pay attention to the lowest order deviation from general theory of relativity in this model by considering this $z = 2$ model.

III. THE GRAND CANONICAL PARTITION FUNCTION FOR RELATIVISTIC PARTICLES IN THE CURVED SPACETIME

We consider the constituent of isothermal spheres as an ideal gas of non-interacting classical particles (which may be celestial bodies). One can write the Hamiltonian of n -particle system in the background spacetime as

$$H_n = N \sum_{a=1}^n \sqrt{\tilde{g}^{ij}p_i^a p_j^a + m^2}. \quad (3.1)$$

where m is the common mass of the particles and p_i^a denotes the momentum of a -th particle located at q_a .

Let us consider the grand canonical formalism for the isothermal system. Then, the grand canonical partition function at the temperature T is written as [23]

$$\begin{aligned} Z_G &= \sum_{n=0}^{\infty} \frac{z^n}{n!} \int \int \prod_{a=1}^n \frac{d^3 p_a d^3 q_a}{(2\pi)^3} e^{-\beta H_n} \\ &= \sum_{n=0}^{\infty} \frac{z^n}{n!} \int \prod_{a=1}^n d^3 q_a \sqrt{\tilde{g}} \frac{m^3}{2\pi^2} \frac{K_2(\beta m N)}{\beta m N} \\ &= \sum_{n=0}^{\infty} \frac{z^n}{n!} \left[\int d^3 q \sqrt{\tilde{g}} \frac{m^3}{2\pi^2} \frac{K_2(\beta m N)}{\beta m N} \right]^n \\ &= \exp \left[\int d^3 x \sqrt{\tilde{g}} \frac{z m^3}{2\pi^2} \frac{K_2(\beta m N)}{\beta m N} \right], \end{aligned} \quad (3.2)$$

where $\beta = 1/T$ and z is the activity. The special function $K_\nu(z)$ is the modified Bessel function of the second kind. Here, the background metric is assumed to be fixed or nearly

constant, for we consider only adiabatic situation or local equilibrium. It should be noted that, in the limiting cases, the expression reduces to be simple as

$$\frac{z m^3 K_2(\beta m N)}{2\pi^2 \beta m N} \approx \begin{cases} z \left(\frac{m}{2\pi\beta N}\right)^{3/2} e^{-\beta m N} & \beta m N \gg 1 \\ \frac{z}{\pi^2(\beta N)^3} & \beta m N \ll 1 \end{cases}. \quad (3.3)$$

It is also noteworthy that the inverse temperature β appears only as the combination $\beta N = \beta\sqrt{-g_{00}}$, as advocated by Tolman [24] in the last century.

Using the partition function, we find that the particle number density is given by

$$n_p = z \frac{\partial}{\partial z} \left[\frac{z m^3 K_2(\beta m N)}{2\pi^2 \beta m N} \right] = \frac{z m^3 K_2(\beta m N)}{2\pi^2 \beta m N}, \quad (3.4)$$

while the pressure of the gas is given by

$$P = \frac{z m^3 K_2(\beta m N)}{2\pi^2 \beta^2 m N^2} = \frac{n_p}{\beta N}, \quad (3.5)$$

and the energy density is given by

$$\rho = -\frac{1}{N} \frac{\partial}{\partial \beta} \left[\frac{z m^3 K_2(\beta m N)}{2\pi^2 \beta m N} \right] = \frac{z m^3}{2\pi^2 \beta N} \left[K_1(\beta m N) + \frac{3K_2(\beta m N)}{\beta m N} \right]. \quad (3.6)$$

It is easy to see that, in the well-known relativistic limit $\beta m \ll 1$, the equation of state becomes $\rho = 3P$. Note that $P/\rho \approx 0.01$ for $\beta m N = 100$, $P/\rho \approx 0.08$ for $\beta m N = 10$, and $P/\rho \approx 0.1$ for $\beta m N = 6$.

IV. THE EQUATIONS FOR ISOTHERMAL SPHERES FROM PARTITION FUNCTION

We consider the total adiabatic system of gravity coupled to isothermal gas. The partition function can be represented by the path integral of the variables if the spacetime is approximately static. We assume that the shift vector vanishes for non-rotating bodies and the integration over conjugate momentum π^{ij} is omitted.³ Then the grand canonical partition function in this system is written as:

$$Z_G = \int [DN][D\tilde{g}_{ij}] \exp \left\{ \int \left[-\beta N \bar{\mathcal{H}} + \frac{z m^3 K_2(\beta m N)}{2\pi^2 \beta m N} \right] \sqrt{\tilde{g}} d^3 x \right\}, \quad (4.1)$$

³ In other words, the graviton degrees of freedom are out of the thermal equilibrium.

where

$$\overline{\mathcal{H}} = -\mu^3 \left[\tilde{R} - \frac{2}{\omega} \left(\tilde{R}^{ij} \tilde{R}_{ij} - \frac{3}{8} \tilde{R}^2 \right) \right]. \quad (4.2)$$

We can derive equations for the static equilibrium configuration. Such equations are obtained by the evaluation of the steepest descend, or the variation of the total Hamiltonian which is described in the exponential in (4.2). One can get the following classical equations of motion from the variational principle:

$$\begin{aligned} \tilde{R} - \frac{2}{\omega} \left(\tilde{R}^{ij} \tilde{R}_{ij} - \frac{3}{8} \tilde{R}^2 \right) &= \frac{zm}{\mu^3} \frac{m^3}{2\pi^2} \frac{1}{\beta m N} \left[K_1(\beta m N) + \frac{3}{\beta m N} K_2(\beta m N) \right] = \frac{1}{\mu^3} \rho, \quad (4.3) \\ N \left\{ \tilde{R}_{ij} - \frac{1}{2} \tilde{R} \tilde{g}_{ij} - \frac{2}{\omega} \left[2\tilde{R}_{ik} \tilde{R}_j^k - \frac{1}{2} \tilde{R}_{kl} \tilde{R}^{kl} \tilde{g}_{ij} - \frac{3}{8} \left(2\tilde{R} \tilde{R}_{ij} - \frac{1}{2} \tilde{R}^2 \tilde{g}_{ij} \right) \right] \right\} \\ - \nabla_i \nabla_j N + \nabla^2 N \tilde{g}_{ij} - \frac{2}{\omega} \left[-\nabla^k \nabla_i (N \tilde{R}_j k) - \nabla^k \nabla_j (N \tilde{R}_i k) + \nabla_k \nabla_l (N \tilde{R}^{kl}) + \nabla^2 (N \tilde{R}_{ij}) \right. \\ \left. - \frac{3}{8} \left(-2\nabla_i \nabla_j (N \tilde{R}) + 2\nabla^2 (N \tilde{R}) \tilde{g}_{ij} \right) \right] &= \frac{z}{2\beta \mu^3} \frac{m^3}{2\pi^2} \frac{K_2(\beta m N)}{\beta m N} \tilde{g}_{ij} = \frac{N}{2\mu^3} P \tilde{g}_{ij}, \quad (4.4) \end{aligned}$$

where $\nabla^2 \equiv \nabla_k \nabla^k$. Incidentally, the trace of (4.4) gives

$$\begin{aligned} -\frac{1}{2} N \tilde{R} + 2\nabla^2 N - \frac{2}{\omega} \left[\frac{1}{2} N \left(\tilde{R}^{ij} \tilde{R}_{ij} - \frac{3}{8} \tilde{R}^2 \right) + (\nabla_k \nabla_l N) \left(\tilde{R}^{kl} - \frac{1}{2} \tilde{R} \tilde{g}^{kl} \right) \right] \\ = \frac{3z}{2\beta \mu^3} \frac{m^3}{2\pi^2} \frac{K_2(\beta m N)}{\beta m N} = \frac{3N}{2\mu^3} P. \quad (4.5) \end{aligned}$$

Note that the general relativistic case can be obtained if $\frac{z}{\omega} \rightarrow 0$. Then, (4.3) and (4.5) give the formal ‘‘classical’’ equation for N :

$$\frac{1}{N} \nabla^2 N = \frac{z}{4\mu^3} \frac{m^4}{2\pi^2 (\beta m N)} \left[K_1(\beta m N) + \frac{6}{\beta m N} K_2(\beta m N) \right] = \frac{1}{4\mu^3} (\rho + 3P). \quad (4.6)$$

The Newtonian limit is attained if $N^2 \approx 1 + 2\phi$, $\tilde{g}_{ij} \approx \delta_{ij}$, $\beta m \gg 1$, and $\mu^3 = \frac{1}{16\pi G}$, where G is the Newton constant. Keeping the lowest order terms, (4.6) leads to

$$\nabla^2 \phi = 4\pi G \rho_0 e^{-\beta m \phi}, \quad (4.7)$$

where we set $\rho_0 \equiv z e^{-\beta m} m \left(\frac{m}{2\pi\beta} \right)^{3/2}$. This equation is already known for the Newtonian isothermal gas [1–5].

Now, we have reached the stage of discussing the case with spherical symmetry. The line element we use is given by

$$ds^2 = -N^2(r) dt^2 + \frac{dr^2}{1 - \frac{2GM(r)}{r}} + r^2 (d\theta^2 + \sin^2 \theta d\varphi^2), \quad (4.8)$$

where $G = \frac{1}{16\pi\mu^3}$ is the Newton constant. The function $M(r)$ will describe the mass inside the sphere with radius r . Substituting the metric (4.8), the equations of motion are reduced to

$$\frac{G}{r^2} \left[1 + \frac{2GM(r)}{\omega r^3} \right] \frac{dM(r)}{dr} - \frac{2}{\omega} \frac{3G^2 M^2(r)}{2r^6} = 4\pi G \rho(r), \quad (4.9)$$

$$\begin{aligned} & \frac{1}{r} \left[1 - \frac{2GM(r)}{r} \right] \left[1 + \frac{2GM(r)}{\omega r^3} \right] \frac{dN(r)}{dr} - \frac{G}{r^3} \left[1 - \frac{2GM(r)}{\omega 2r^3} \right] M(r)N(r) \\ & = 4\pi GNP(r), \end{aligned} \quad (4.10)$$

where $\rho(r)$ and $P(r)$ are defined by (3.6) and (3.5) with $N \rightarrow N(r)$. Note that the second or higher derivative of functions are eliminated. In order to simplify the equations further, we make a rescaling of variables,

$$x \equiv \sqrt{4\pi G \rho_c} r, \quad y \equiv \beta m N, \quad \tilde{M} \equiv \sqrt{4\pi G \rho_c} GM, \quad \alpha \equiv 4\pi G \rho_c \frac{2}{\omega}, \quad (4.11)$$

with

$$\rho_c \equiv \frac{z m^4}{2\pi^2 y_0} \left[K_1(y_0) + \frac{3K_2(y_0)}{y_0} \right], \quad y_0 \equiv y(0). \quad (4.12)$$

Then, the equations for $y(x)$ and $\tilde{M}(x)$ become

$$\frac{1}{x^2} \left(1 + \alpha \frac{\tilde{M}}{x^3} \right) \tilde{M}' - \alpha \frac{3\tilde{M}^2}{2x^6} = \frac{y_0}{y} \frac{K_1(y) + \frac{3K_2(y)}{y}}{K_1(y_0) + \frac{3K_2(y_0)}{y_0}}, \quad (4.13)$$

$$\frac{1}{x} \left(1 - \frac{2\tilde{M}}{x} \right) \left(1 + \alpha \frac{\tilde{M}}{x^3} \right) y' - \frac{1}{x^3} \left(1 - \alpha \frac{\tilde{M}}{2x^3} \right) \tilde{M} y = \frac{y_0}{y} \frac{K_2(y)}{K_1(y_0) + \frac{3K_2(y_0)}{y_0}}, \quad (4.14)$$

where the prime (') means the derivative with respect to x . We must find solutions satisfying the boundary conditions

$$\tilde{M}(0) = 0, \quad y(0) = y_0. \quad (4.15)$$

In the next section, we exhibit the numerical results.

V. NUMERICAL CALCULATIONS

A. General relativistic isothermal spheres

First, we consider general relativistic isothermal sphere, i.e., in the case with $\alpha = 0$. We define two functions:

$$u \equiv \frac{r}{M(r)} \frac{dM(r)}{dr} = x \frac{\tilde{M}'(x)}{\tilde{M}(x)}, \quad v \equiv \beta m r \frac{dN(r)}{dr} = xy'(x). \quad (5.1)$$

Note that the Newtonian limit of v yields

$$v = \beta m r \frac{dN(r)}{dr} = (\beta m N) \frac{r}{N(r)} \frac{dN(r)}{dr} \rightarrow \frac{\rho(r)}{P(r)} r \frac{d\phi(r)}{dr} \approx \frac{\rho(r)}{P(r)} \frac{GM(r)}{r}, \quad (5.2)$$

where ϕ denotes the Newtonian gravitational potential.

In Fig. 1, we show the solutions for various initial conditions in the (u, v) -plane. The black curve indicates the Newtonian isothermal sphere [1]. The curves in red, blue, and cyan correspond to the boundary conditions $y_0 = 100$, 10, and 6, respectively. All the curves start at the point $(u, v) = (3, 0)$, which represents the center of the isothermal sphere, and approach the fixed point $(u, v) \approx (1, 2)$, which corresponds to $x \rightarrow \infty$. In our present model, since the equation of state in the asymptotic region $x \gg 1$ becomes non-relativistic one as the density decreases, the behavior $M(r) \propto r$ is the same as in the case of the Newtonian isothermal sphere [1–5].

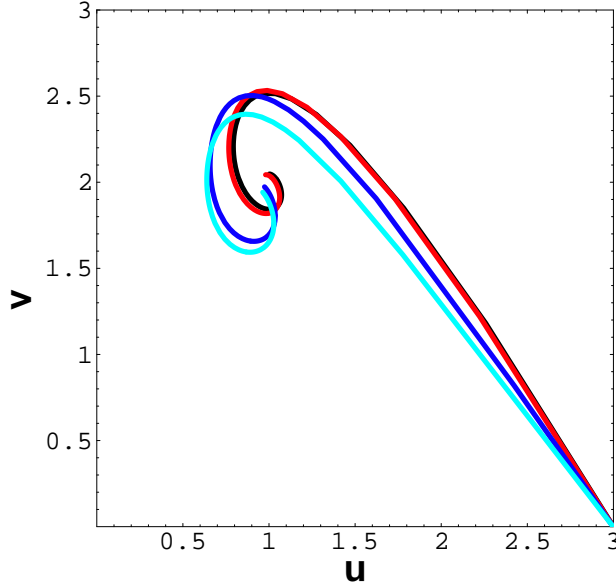


FIG. 1. The (u, v) curves for $y_0 = 100$ (red), $y_0 = 10$ (blue), and $y_0 = 6$ (cyan). The black curve indicates the Newtonian isothermal sphere.

The behavior of curves near $(u, v) = (3, 0)$ is found to be

$$u = 3 + bv, \quad (v \ll 1) \quad (5.3)$$

where

$$b = -\frac{3 \left[\frac{3}{y_0} K_1(y_0) + \left(1 + \frac{12}{y_0^2}\right) K_2(y_0) \right]}{5 \left[K_1(y_0) + \frac{3}{y_0} K_2(y_0) \right]} \approx \begin{cases} -\frac{3}{5} & (y_0 \gg 1) \\ -\frac{12}{5y_0} & (y_0 \ll 1) \end{cases}. \quad (5.4)$$

Fig. 2 is the plot of b against y_0 .

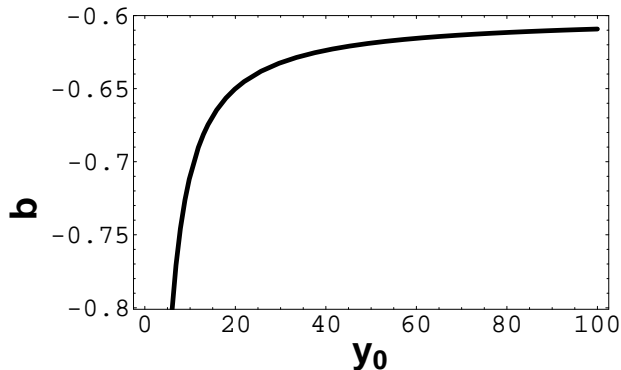


FIG. 2. The slope coefficient b versus y_0 .

Fig. 3 shows the density profiles $\rho(x)/\rho_c$ as functions of $x \propto r$, where the curves in red, blue, and cyan correspond to the boundary conditions $y_0 = 100$, 10, and 6, respectively. In all of the cases, we find the asymptotic behavior $\rho \propto 1/r^2$ similarly to that of the Newtonian isothermal sphere which extends to infinity. Incidentally, it turns out that the asymptotics $v \approx 2$ reads $y \approx 2 \ln x$.

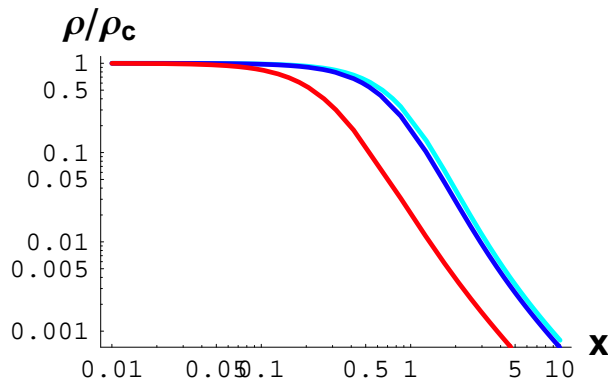


FIG. 3. The density profiles $\rho(x)/\rho_c$ of general relativistic isothermal spheres for $y_0 = 100$ (red), $y_0 = 10$ (blue), and $y_0 = 6$ (cyan).

B. Isothermal spheres in Hořava gravity

Next, we consider the isothermal spheres in Hořava gravity.

The spirals of solutions in the (u, v) -plane is shown in Fig. 4. The fixed point $(u, v) \approx (1, 2)$ is almost unchanged.

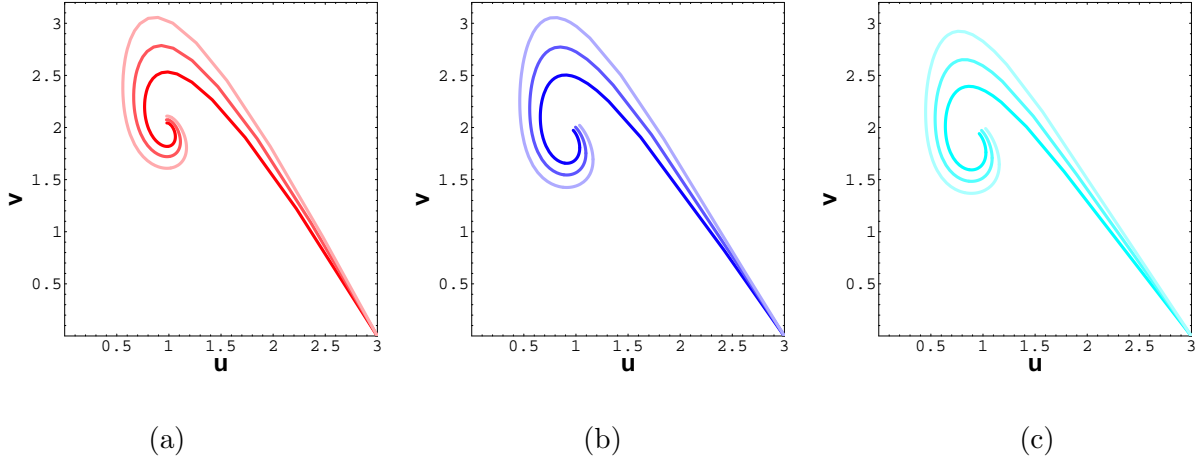


FIG. 4. Plots of spirals in the (u, v) -plane. (a) $y_0 = 100$. (b) $y_0 = 10$. (c) $y_0 = 6$. From the inner spiral to the outer spiral, they indicate $a = 0$, $a = 0.5$, and $a = 1$ in each plot.

Near the starting point, $(u, v) = (3, 0)$, the curve is approximated as

$$u = 3 + bv, \quad (v \ll 1) \quad (5.5)$$

where

$$b = -\frac{3\left(1 + \frac{2\alpha}{3} + \sqrt{1 + \frac{2\alpha}{3}}\right)}{10\left(1 + \frac{2\alpha}{3}\right)} \frac{\frac{3}{y_0}K_1(y_0) + \left(1 + \frac{12}{y_0^2}\right)K_2(y_0)}{K_1(y_0) + \frac{3}{y_0}K_2(y_0)} \approx \begin{cases} -\frac{3\left(1 + \frac{2\alpha}{3} + \sqrt{1 + \frac{2\alpha}{3}}\right)}{10\left(1 + \frac{2\alpha}{3}\right)} & (y_0 \gg 1) \\ -\frac{6\left(1 + \frac{2\alpha}{3} + \sqrt{1 + \frac{2\alpha}{3}}\right)}{5\left(1 + \frac{2\alpha}{3}\right)y_0} & (y_0 \ll 1) \end{cases}. \quad (5.6)$$

Thus, the spirals become larger according to increase of the value of α . The curves in the low-density case with $y_0 = 100$ are given in Fig. 4(a). The relatively high-density cases with $y_0 = 10$ (Fig. 4(b)) and $y_0 = 6$ (Fig. 4(c)) exhibits similar characteristics. The coefficient b is plotted against α and y_0 in Fig. 5.

The profiles of the energy density for $\alpha = 0.5$ and 1 are shown in Fig. 6. Note that here ρ is defined by $\propto \frac{1}{4\pi r^2} \frac{dM(r)}{dr}$. They seem to have similar behavior to the case in general relativity ($\alpha = 0$). This is because the terms with the coefficient α in the equations is proportional to M/r^3 and this behaves asymptotically $\propto 1/r^2$ for $r \rightarrow \infty$. In other words, all isothermal spheres in our present model have the outer region which is well described by the structure of the Newtonian isothermal spheres.

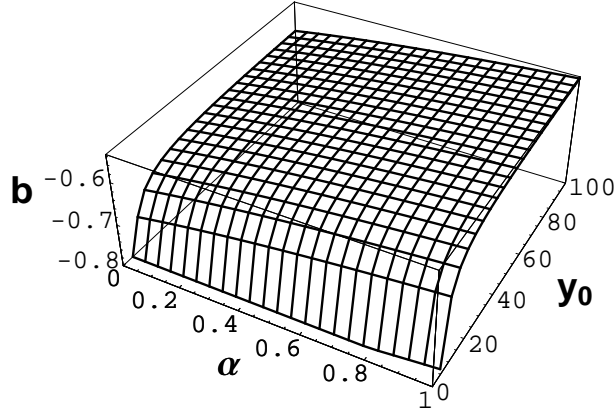


FIG. 5. The slope coefficient b is plotted against α and y_0 .

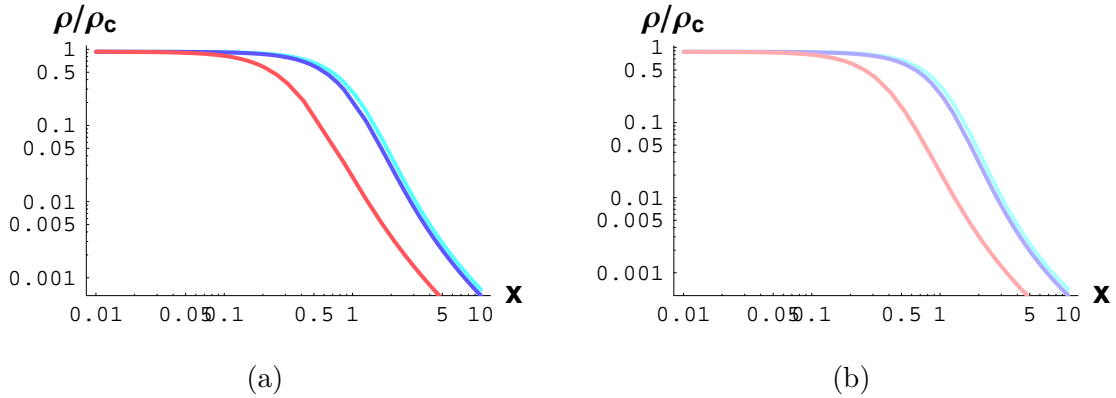


FIG. 6. The density profiles $\rho(x)/\rho_c$ for $y_0 = 100$ (red), $y_0 = 10$ (blue), and $y_0 = 6$ (cyan) with the parameter $\alpha = 0.5$ are plotted in (a) while those are plotted with $\alpha = 1$ in (b).

C. Stability

While the behavior of the spirals in the (u, v) -plane and the density profiles have moderate dependence on the central density and the parameter α which appears in Hořava gravity, the parameter dependence of stability is very complicated as we will show below. Therefore, in the present paper, we only discuss the stability by considering the ratio of the sum of the mass of constituent particles and the mass of the isothermal sphere in the region of the fixed radius. The analyses using various known method are left for future studies.

Because the isothermal spheres in our model have the same asymptotic density profile as the Newtonian one, we consider the finite spherical box to define the mass of the object

[1–5]. We consider the region inside the sphere with radius r .

We here consider the ratio mN_p/M , where

$$N_p = 4\pi \int_0^r n_p(r) \frac{r^2}{\sqrt{1 - \frac{2GM(r)}{r}}} dr = \frac{1}{G\sqrt{4\pi G\rho_c}} \int_0^x \frac{y_0 K_2(y(x'))}{y(x')[(K_1(y_0) + \frac{3}{y_0} K_2(y_0))]} \frac{x'^2}{\sqrt{1 - \frac{2\tilde{M}(x')}{x'}}} dx'. \quad (5.7)$$

Then, the ratio can be expressed as

$$\frac{mN_p}{M} = \frac{1}{\tilde{M}(x)} \int_0^x \frac{y_0 K_2(y(x'))}{y(x')[(K_1(y_0) + \frac{3}{y_0} K_2(y_0))]} \frac{x'^2}{\sqrt{1 - \frac{2\tilde{M}(x')}{x'}}} dx'. \quad (5.8)$$

Fig. 7 shows the ratio mN_p/M against $-\log_{10}[\rho/\rho_c]$. Since the ratio $\rho(r)/\rho_c$ monotonically decrease with r , as we have seen in this section, the radius of spherical box becomes larger from left to right in the horizontal axis. Notice that, apart from some exception, the characteristic feature of plots lies inside the finite region by selecting the scale of the axis.

Since $N_p = \int n_p \sqrt{g} d^3x$, the ratio $mN_p/M > 1$ means the negative binding energy, so the isothermal sphere is expected to be energetically stable in this case.

We should also consider the maximum point of the ratio. At the right-hand side of the maximum, increase of the radius of sphere reduces the amount of the binding energy per mass. Thus, there appears the possibility that some smaller bodies produced by fission will be more stable than a single body.

In Fig. 7(a), we show the general relativistic case ($\alpha = 0$). If the central density is sufficiently large (i.e., the gas is rather relativistic in the vicinity of the center), the stable configuration disappears according to the above-mentioned criteria. Its critical value is $y_0 \approx 7.8$. The change of the curve is however complicated for $y_0 > 10$. For $y_0 = 100$, the maximum is located around $-\log_{10}[\rho(r)/\rho_c] \approx 2.5$. This is consistent with the known stability criterion for the Newtonian isothermal sphere $-\log_{10}[\rho(r)/\rho_c] < 2.85$ [3–5].

The case with the Hořava-type gravity is more complicated. The behaviors of curves in Fig. 7(b) (for $\alpha = 0.5$), (c) (for $\alpha = 1$) are drastically changed if y_0 is larger than about 10. This is because the terms including α in (4.13) and (4.14), which have finite values in the central region (i.e., $\tilde{M}(x)/x^3 = \frac{2}{3+\sqrt{9+6\alpha}} + O(x^2)$ if $x \ll 1$), are dominant over the contribution of densities in the right-hand side of the equations in the small scale. Thus, the almost non-relativistic gas sphere is stable when the radius is relatively small. Another important feature one can observe in Fig. 7 is that even the relatively high-central-density spheres may possess a stable radius if α is sufficiently large.

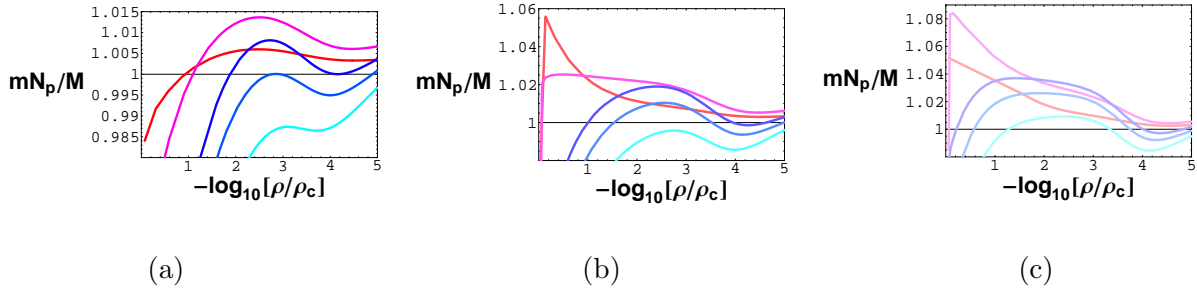


FIG. 7. The ratio mN_p/M is plotted. (a) $a = 0$. (b) $a = 0.5$. (c) $a = 1$. In each plot, the curve in red represents for $y_0 = 100$, in magenta for $y_0 = 30$, in blue for $y_0 = 10$, in pale blue for $y_0 = 7.8$, and in cyan for $y_0 = 6$.

VI. CONCLUSION

In this paper, we investigated isothermal spheres in general relativity and in a concise version of the Hořava gravity model. We concentrated ourselves on spherically symmetric and static solutions of the equations for the locally equilibrium configuration. We found that the non-relativistic limit reproduces the already known Newtonian isothermal sphere.

We found that the stability of the sphere tends to be spoiled by the high density at the center of the general relativistic isothermal sphere. In the Hořava-type gravity, the higher-derivative term stabilize the sphere even if the central density is rather high; however, at the same time, the term makes the radius of the stable sphere vary small with low central density.

In vacuum, the value of the parameter of the Hořava gravity is severely limited observationally [25]. Recalling that, however, the parameter α is defined as $4\pi G\rho_c\frac{2}{\omega}$ and it is enhanced in the matter in general. Thus, considering the higher-derivative correction is meaningful in study of the general high-density stellar structure. The study with various modified gravitational theories and with other choices of equations of state should be a topic for the future.

We also continue discussing the stability from various point of view, including thermodynamical aspects, and we shall report such analyses in a future work.

Last but not least, we have intended to approach finite-temperature self-gravitating system from first principles. Further development of theoretical study in this line, including extension to non-extensive statistical dynamics [26–28] and generalization of canonically-

formulated gravity [29, 30], will be reported elsewhere.

-
- [1] S. Chandrasekhar, “Introduction to the study of stellar structure” (Dover, New York, 1939).
 - [2] J. Binney and S. Tremaine, “Galactic Dynamics” (Princeton Univ. Press, Princeton, 1987).
 - [3] V. A. Antonov, “Most probable phase transition in spherical star systems and conditions for its existence”, *Vest. Leningr. gos. Univ.* **7** (1962) 135; *IAU Symposia* **113** (1985) 525.
 - [4] D. Lynden-Bell and R. Wood, “The gravo-thermal catastrophe in isothermal spheres and the onset of red-giant structure for stellar systems”, *Mon. Not. R. Astron. Soc.* **138** (1968) 495.
 - [5] T. Padmanabhan, “Statistical mechanics of gravitating systems”, *Phys. Rep.* **188** (1990) 285.
 - [6] G. Bertone, D. Hooper and J. Silk, “Particle dark matter: Evidence, candidates and constraints”, *Phys. Rep.* **405** (2005) 279.
 - [7] S. Profumo, “An Introduction to Particle Dark Matter” (World Scientific, Singapore, 2017).
 - [8] T. Clifton, P. G. Ferreira, A. Padilla and C. Skordis, “Modified Gravity and Cosmology”, *Phys. Rep.* **513** (2012) 1.
 - [9] S. Capozziello and M. De Laurentis, “Extended Theories of Gravity”, *Phys. Rep.* **509** (2011) 167.
 - [10] P. Hořava, “Membrane at quantum criticality”, *JHEP* **0903** (2009) 020.
 - [11] P. Hořava, “Quantum gravity at a Lifshitz point”, *Phys. Rev.* **D79** (2009) 084008.
 - [12] G. J. Olmo, D. Rubiera-Garcia and A. Wojnar, “Stellar structure models in modified theories of gravity: Lessons and Challenges”, *Phys. Rep.* **876** (2020) 1.
 - [13] J. Sommer-Larsen, H. Vedel and U. Hellsten, “The structure of isothermal, self-gravitating, stationary gas spheres for softened gravity”, *ApJ* **500** (1998) 610.
 - [14] A. Giusti, “MOND-like fractional Laplacian theory”, *Phys. Rev.* **D101** (2020) 124029.
 - [15] A. Giusti, R. Garrappa and G. Vachon, “On the Kuzmin model in fractional Newtonian gravity”, arXiv:2009.04335 [gr-qc].
 - [16] Z. F. Seidov, “Non- $1/r$ Newtonian gravitation and stellar structure”, astro-ph/9907136.
 - [17] M. Lazar, “Gradient modification of Newtonian gravity”, arXiv:2009.09846 [gr-qc].
 - [18] A. Wang, “Horava gravity at a Lifshitz point: a progress report”, *Int. J. Mod. Phys.* **D26** (2017) 1730014.
 - [19] Y. S. Myung, Y.-W. Kim, W.-S. Son and Y.-J. Park, “Chaotic universe in the $z = 2$ Hořava–

- Lifshitz gravity”, Phys. Rev. **D82** (2010) 043506.
- [20] Y. S. Myung, “Chiral gravitational waves from $z = 2$ Hořava–Lifshitz gravity”, Phys. Lett. **B684** (2010) 1.
- [21] A. Kehagias and K. Sfetsos, “The black hole and FRW geometries of non-relativistic gravity”, Phys. Lett. **B678** (2009) 123.
- [22] R. L. Arnowitt, S. Deser and C. W. Misner, “Canonical variables for general relativity”, Phys. Rev. **117** (1960) 1595. Gen. Rel. Grav. **40** (2008) 1997.
- [23] W. Greiner, L. Neise and H. Stöcker, “Thermodynamics and statistical mechanics” (Springer-Verlag, New York, 1995).
- [24] R. C. Tolman, “Relativity, thermodynamics, and cosmology” (Dover, New York, 1987).
- [25] T. Harko, Z. Kovács and F. S. N. Lobo, “Solar system tests of Hořava–Lifshitz gravity” Proc. R. Soc. **A467** (2011) 1390.
- [26] A. Taruya and M. Sakagami, “Gravothermal catastrophe and Tsallis’ generalized entropy of self-gravitating systems”, Physica **A307** (2002) 185.
- [27] A. Taruya and M. Sakagami, “Gravothermal catastrophe and Tsallis’ generalized entropy of self-gravitating systems. (II). Thermodynamic properties of stellar polytrope”, Physica **A318** (2003) 387.
- [28] A. Taruya and M. Sakagami, “Gravothermal catastrophe and Tsallis’ generalized entropy of self-gravitating systems. (III). Quasi-equilibrium structure using normalized q -values”, Physica **A322** (2003) 285.
- [29] S. Mukohyama and K. Noui, “Minimally modified gravity: a Hamiltonian construction”, JCAP **1907** (2019) 049.
- [30] K. Aoki, A. De Felice, S. Mukohyama, K. Noui, M. Oliosi and M. C. Pookkillath, “Minimally modified gravity fitting Planck data better than λ CDM”, Eur. Phys. J. **80** (2020) 708.